Cell Reports

Report

Structural Studies Reveal the Functional Modularity of the Scc2-Scc4 Cohesin Loader

Graphical Abstract

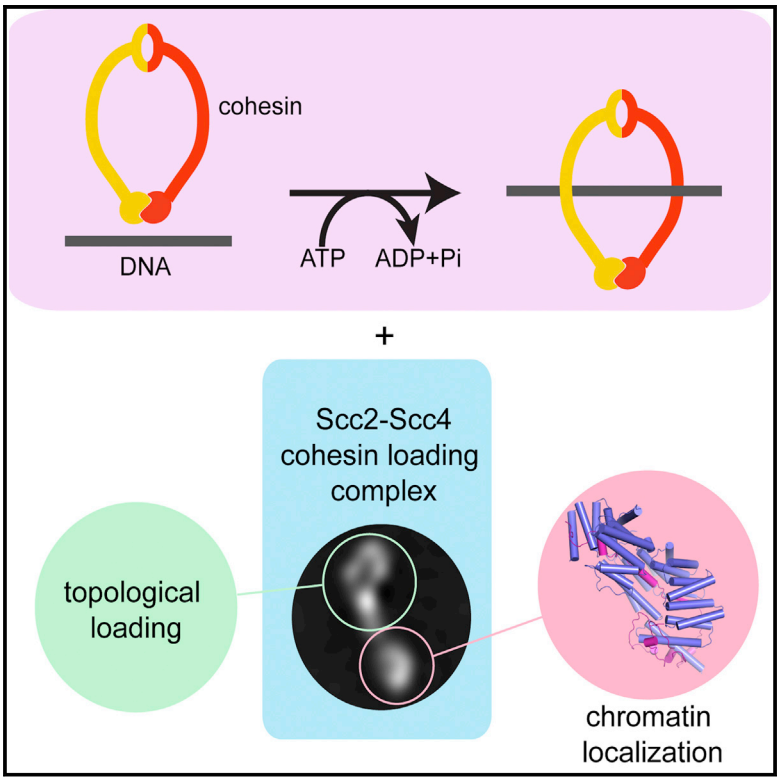

Authors

William C.H. Chao, Yasuto Murayama, Sofía Muñoz, Alessandro Costa, Frank Uhlmann, Martin R. Singleton

Correspondence

martin.singleton@crick.ac.uk

In Brief

Chao et al. report a structural and functional analysis of the Scc2-Scc4 complex that topologically loads cohesin rings onto chromosomes. The Scc4 protein forms an independent domain that is required to bind chromatin, whereas Scc2 forms a prominent flexible hook that undergoes conformational transitions possibly involved in the loading reaction.

Highlights

- Scc4 forms a tetratricopeptide repeat barrel encapsulating the Scc2 N terminus
- Electron microscopy shows the Scc2-Scc4 complex is highly flexible.
- The Scc2 C-terminal domain is sufficient to catalyze cohesin loading

Accession Numbers

5C6G

Chao et al., 2015, Cell Reports *12*, 719–725
August 4, 2015 ©2015 The Authors
http://dx.doi.org/10.1016/j.celrep.2015.06.071

Cell Reports
Report

Structural Studies Reveal the Functional Modularity of the Scc2-Scc4 Cohesin Loader

William C.H. Chao,[1] Yasuto Murayama,[1] Sofía Muñoz,[1] Alessandro Costa,[2] Frank Uhlmann,[1] and Martin R. Singleton[1,*]
[1]Lincoln's Inn Fields Laboratory, The Francis Crick Institute, 44 Lincoln's Inn Fields, London WC2A 3LY, UK
[2]Clare Hall Laboratory, The Francis Crick Institute, Blanche Lane, South Mimms, Hertfordshire EN6 3LD, UK
*Correspondence: martin.singleton@crick.ac.uk
http://dx.doi.org/10.1016/j.celrep.2015.06.071

SUMMARY

The remarkable accuracy of eukaryotic cell division is partly maintained by the cohesin complex acting as a molecular glue to prevent premature sister chromatid separation. The loading of cohesin onto chromosomes is catalyzed by the Scc2-Scc4 loader complex. Here, we report the crystal structure of Scc4 bound to the N terminus of Scc2 and show that Scc4 is a tetratricopeptide repeat (TPR) superhelix. The Scc2 N terminus adopts an extended conformation and is entrapped by the core of the Scc4 superhelix. Electron microscopy (EM) analysis reveals that the Scc2-Scc4 loader complex comprises three domains: a head, body, and hook. Deletion studies unambiguously assign the Scc2N-Scc4 as the globular head domain, whereas in vitro cohesin loading assays show that the central body and the hook domains are sufficient to catalyze cohesin loading onto circular DNA, but not chromatinized DNA in vivo, suggesting a possible role for Scc4 as a chromatin adaptor.

INTRODUCTION

In eukaryotes, genomic integrity during cell-cycle division is safeguarded by cohesin, a macromolecular complex consisting of subunits Smc1, Smc3, Scc1, and Scc3. The Smc subunits of cohesin contain long coiled coils that form a ring structure that is believed to topologically entrap sister chromatids (Haering et al., 2008). This linking is required to ensure that the two chromatids are correctly segregated in a bi-polar manner. Upon anaphase onset, cohesin is proteolytically cleaved at its Scc1 subunit, leading to the relief of physical constraint between the sister chromatids and allowing separation of the genome. As well as its role in sister chromatid cohesion, cohesin also functions in DNA double-strand break repair (Lightfoot et al., 2011) as well as in transcription regulation (Kagey et al., 2010) and execution of developmental programs (Dorsett, 2011). The Scc2-Scc4 complex plays an essential role in these functions and is required to ensure that cohesin is loaded at its required destination at the correct time (Ciosk et al., 2000; Gillespie and Hirano, 2004; Lengronne et al., 2004; Watrin et al., 2006).

The Scc2-Scc4 complex was initially described as the universal loading factor of cohesin (Ciosk et al., 2000). Scc2 is a HEAT repeat protein (Neuwald and Hirano, 2000) that has been shown to catalyze cohesin loading onto circular (topologically closed) DNA in vitro (Murayama and Uhlmann, 2014). The human homolog of Scc2, Nipbl, has been shown to form a complex with cohesin and the Mediator complex that connects enhancers and promoters of actively transcribing genes (Kagey et al., 2010). Mutations in the Nipbl^{Scc2} are present in 60% of patients with Cornelia de Lange syndrome (CdLS), which belongs to a family of hereditary diseases known as cohesinopathies (Krantz et al., 2004; Tonkin et al., 2004). These diseases are characterized by abnormal gene expression, driven by loss-of-function mutations of cohesin subunits and its loader, Nipbl^{Scc2}.

The function of the tetratricopeptide repeat (TPR) Scc4 subunit (Mau2 in humans) is less well defined, but it is thought to be responsible for the recruitment of Scc2 to specific locations on chromosomes (Bernard et al., 2006; Seitan et al., 2006; Watrin et al., 2006). It has been shown in *Xenopus* egg extracts that Scc2 is recruited to pre-replication complex (preRC) via Scc4 through its interaction with the Cdc7-Dbf4 kinase (Takahashi et al., 2008). In yeast, the pericentromeric localization of Scc2-Scc4 complex depends on the Cft19 kinetochore complex as well as intact cohesin (Fernius et al., 2013; Natsume et al., 2013). More recently, chromatin immunoprecipitation (ChIP) analysis has revealed that the Scc2-Scc4 complex is recruited to broad nucleosome-free regions by remodeling the structure of chromatin (RSC) complex at promoter regions of actively transcribing genes and plays an essential role in maintaining the DNA morphology in these regions (Lopez-Serra et al., 2014). In short, depending on the final destination of cohesin, there seem to be multiple pathways through which chromosome recruits the Scc2-Scc4.

In order to better understand how the Scc2-Scc4 complex functions as a cohesin loader, we have determined the crystal structure of Scc4 bound to the interacting section of Scc2. Together with electron microscopy (EM) analysis of the intact complex, in vitro cohesin loading assays, and in vivo chromatin-binding assays, we demonstrate the modular nature of the Scc2-Scc4 complex and shed light on how these modules function in a coordinated manner to bring about cohesin targeting and loading onto chromosomes.

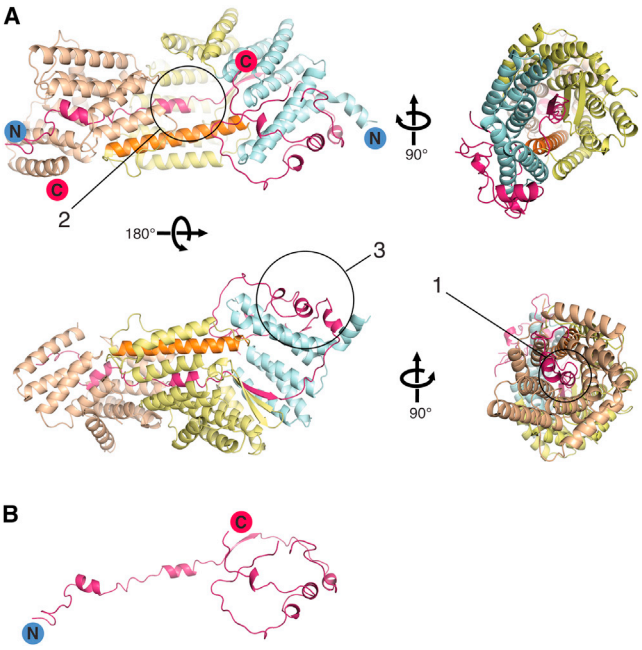

Figure 1. Structure of the Scc2N-Scc4 Complex

(A) Scc2N-Scc4 adopts an anti-parallel conformation with the right-handed TPR superhelix of Scc4 enclosing Scc2N as an extended structure connected to an external C-terminal domain. Scc4 is divided into three TPR domains. The N-terminal domain (pale blue) is sandwiched by the external C-terminal domain of Scc2N and a central Scc2 β strand (purple). The central Scc4 domain (yellow) forms a tunnel (1) with a long helix (orange) to accommodate the Scc2N central short helix. The central Scc2 helical segment is exposed to solvent via a large cavity created by the separation of the N-terminal and central domains of Scc4 (2). The C-terminal Scc4 TPR superhelix (tan) deforms significantly to allow the exit of the N terminus of Scc2N. The external domain of Scc2 contains a short three-helix segment that sits on a ledge formed by the Scc4 N-terminal (3).

(B) The Scc2 N-terminal in isolation, highlighting its extended nature.

RESULTS

Structure Determination

We generated an initial full-length *Ashbya gossypii* Scc2-Scc4 complex by co-expressing Scc2 with Scc4 in a modified baculovirus expression system (Zhang et al., 2013). Proteolytic products of both proteins were observed in the purified samples and were subsequently identified by mass spectrometry and Edman sequencing. Two constructs were re-cloned based on the following results: (1) $Scc2^{1–168}$-$Scc4^{34–620}$ (hereon Scc2N-Scc4) and (2) $Scc2^{168–1,479}$-$Scc4^{34–620}$ (Scc2C-Scc4). Only Scc2N-Scc4 showed a stoichiometric complex between the Scc2N and Scc4 subunits, indicating that the N terminus of Scc2 alone is sufficient in mediating Scc4 interaction. Crystals of Scc2N-Scc4 were grown and diffracted to 2.6 Å resolution. The structure was determined experimentally by multiwavelength anomalous dispersion (MAD) methods (Experimental Procedures).

Scc2N-Scc4 Is a Right-Handed TPR Superhelix

The 95-kDa Scc2N-Scc4 structure adopts an anti-parallel conformation between the two subunits with the right-handed TPR superhelix of Scc4 enclosing Scc2N as an extended structure in its largely hydrophobic central tunnel. Scc4 contains 12 TPR motifs that are characterized into three structurally distinct domains (Figure 1A). The N-terminal domain of Scc4, TPR1–TPR3, is sandwiched by the external C-terminal domain of Scc2N and its central β strand. The central domain of Scc4, TPR4–TPR7, forms a tunnel with a long helix to accommodate the Scc2N central short helix. This central helical segment of Scc2N is curiously exposed to solvent via a large cavity created by the separation of the N-terminal and central domains of Scc4. A hairpin between TPR6 and TPR7 provides an additional contact with Scc2N by forming with it a contiguous β sheet. The TPR8-TPR12 motifs complete the C-terminal domain of Scc4 with the superhelix deforming significantly from TPR10 to TPR12 to provide an exit for the N terminus of Scc2N.

The Scc2 N terminus interacts extensively with the inner surface of the Scc4 TPR barrel, and an additional C-terminal domain of Scc2N covering the exterior Scc4 surface further strengthens the binding. Scc2 folds into four short helices, three of which are packed onto a "ledge" formed by the first TPR repeat. These two binding sites together form an overall buried interaction area of 6,082 $Å^2$. The extended contact between the two proteins promotes high-affinity binding and explains why Scc2 and Scc4 are always observed as a constitutively stable complex (Ciosk et al., 2000; Takahashi et al., 2008; Woodman et al., 2014). The Scc2 N terminus is likely disordered in the absence of Scc4 binding, with the secondary structure elements observed (Figure 1B) only arising on complex formation.

Surface Properties and Conservation

Scc4 orthologs are less well conserved than those of Scc2, but secondary structure predictions and functional considerations would suggest that they all adopt a similar structure. Analysis of the surface conservation of fungal Scc4 orthologs reveals two noteworthy patches (Figure 2A). The first is formed by the exterior Scc2-binding surface and immediately adjacent area, which may participate in more extensive interactions with intact Scc2. The second is on the reverse face of the protein and is lysine rich. These lysines are donated by two separate conserved sections of sequence (Figure 2B) and form a prominent groove. The possible significance of this feature is discussed later.

Structural Implication of CdLS Mutations on the Scc2N C-Terminal Domain

Aligning Scc2N with the human Nipbl extreme N terminus revealed that the external C-terminal domain of Scc2N harbors two documented CdLS mutations (HsNipbl N50I and G90V) (Kuzniacka et al., 2013) (Figure 2C). From a structural point of view, these mutations are unlikely to cause a dissociation of Scc2 from Scc4 in CdLS patients due to the extensive contact between the subunits (Figure 2D). Interestingly, the entire Scc2 N terminus, residues 1–191 in *Schizosaccharomyces pombe*, is not required for efficient loading of cohesin onto plasmid DNA in vitro (Figures 3A–3C). Recombinantly purified *S. pombe* $Scc2C^{192–1,587}$ is sufficient to catalyze cohesin loading with efficiency identical to full-length Scc2-Scc4 complex. CdLS mutations in this Scc2N region are therefore unlikely to affect the loading reaction per se. Recently, studies in vertebrate CdLS

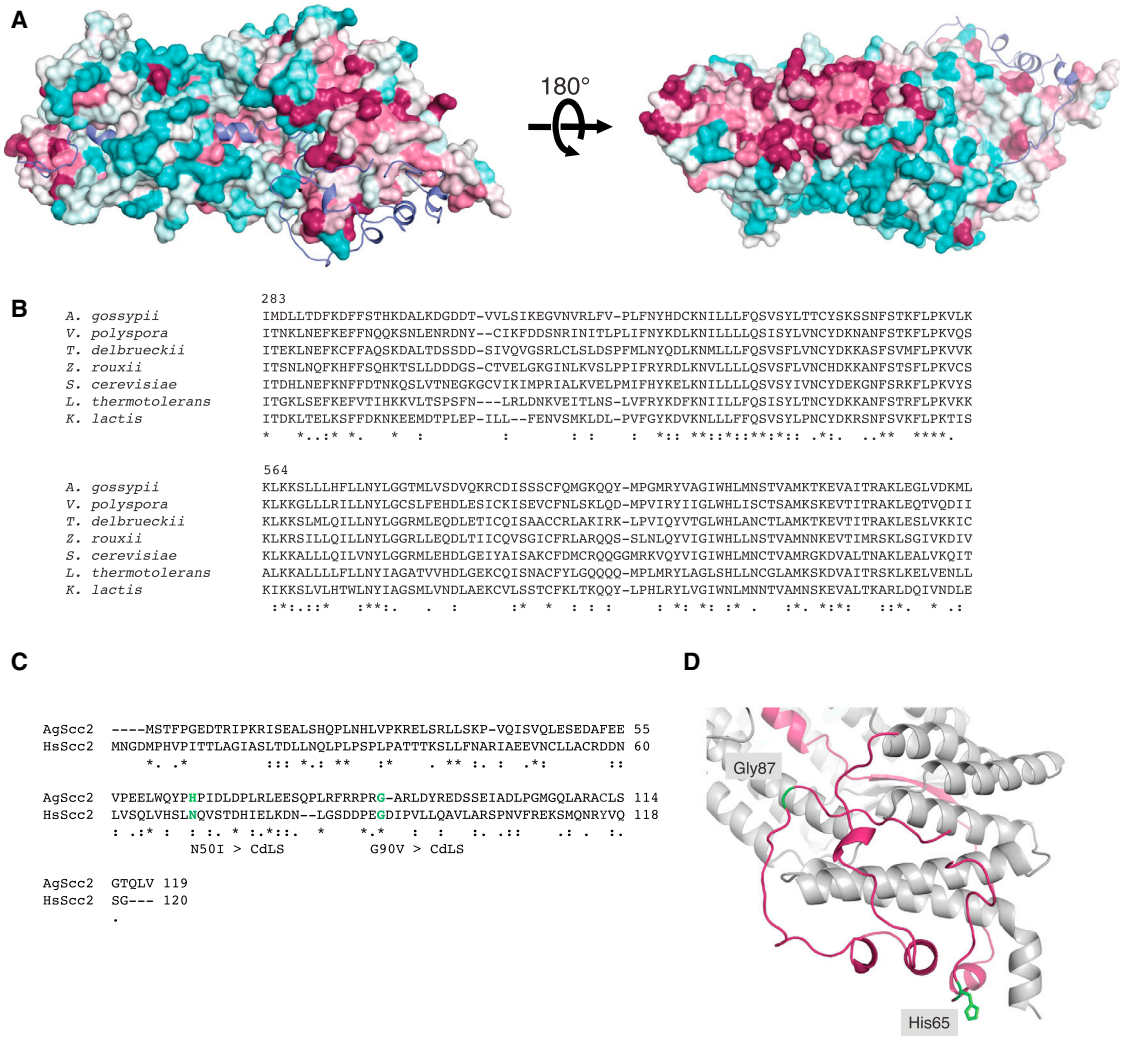

Figure 2. Structural Conservation and CdLS Mutations

(A) Principle areas of surface conservation on Scc4 occur at the Scc2 exterior binding surface, and along a large groove on the reverse face of the protein.

(B) The location of the conserved residues in the primary structure is shown a sequence alignment of fungal Scc4 homologs. Totally conserved residues are indicated with an asterisk.

(C) Sequence alignment between the extreme N termini of *A. gossypii* Scc2 and human Nipbl. CdLS mutations are indicated in green.

(D) Two CdLS mutations with residues conserved between human and *A. gossypii* can be found in the external domain of Scc2N. Gly87 (human Gly90) confers an abrupt bending of an extended loop spanning a large surface of Scc4. A CdLS mutation to valine of this residue would reduce the propensity of this loop to adopt such a conformation, potentially affecting the structural integrity of the Scc2N external domain and disrupting interactions between the Scc2-Scc4 and its binding partners. His65 (human N50) is a solvent-facing residue, which may facilitate polar interaction with partners.

models showed that combined partial reduction of Nipbl and Med12, a subunit of the Mediator complex, has a synergistic effect on limb development and gene expression (Muto et al., 2014). It is plausible that instead of disrupting the Scc2-Scc4 association, the CdLS mutations in the Scc2N C-terminal domain affect binding of the Scc2-Scc4 complex to chromosome receptors such as the Mediator complex and, as a result, cause transcription misregulation via resultant downstream effects.

Scc4 Is Required for Chromatin Targeting In Vivo

To better understand the function of Scc4, we expressed a similarly N-terminally truncated Scc2C$^{126–1,493}$ variant lacking its Scc4 interacting sequence in budding yeast cells. Endogenous Scc2 in these cells could be depleted by an auxin-inducible degron (Nishimura et al., 2009). A chromatin fractionation experiment revealed that interaction with Scc4 is required for efficient Scc2 recruitment to chromatin in vivo, as Scc2C$^{126–1,493}$ was no longer detected in the chromatin fraction compared to full-length Scc2 (Figure 3D). Probably as a consequence, Scc2C$^{126–1,493}$ was unable to support cohesin loading onto chromatin. This suggests that interaction with Scc4 is crucial for the function of the cohesin loader in a chromatin context in vivo. To test whether Scc4 simply targets chromatin by directly binding DNA, we performed a gel

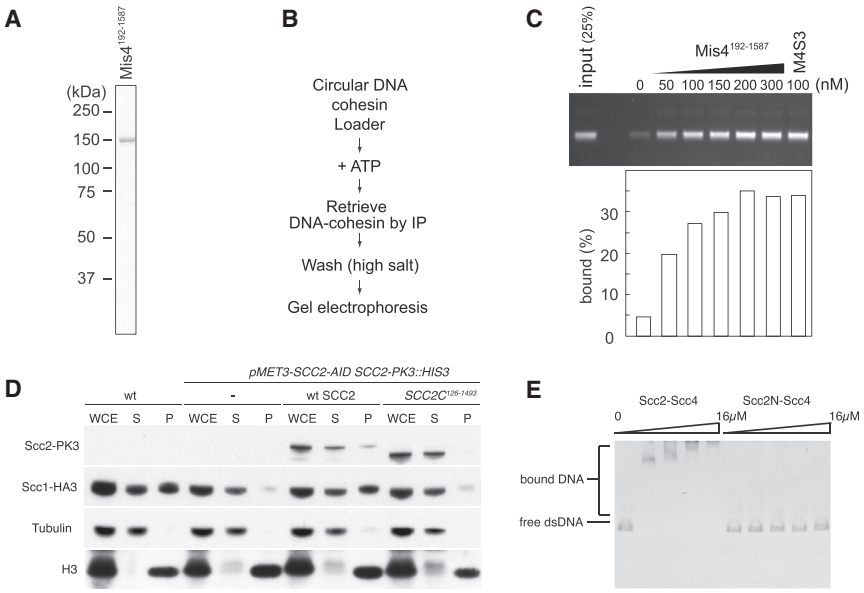

Figure 3. The C Terminus of Scc2 Promotes DNA Entrapment by the Cohesin Ring, whereas Scc4 Is Required for Chromatin Binding

(A) The purified fission yeast Scc2C$^{192–1,587}$ (Mis4C$^{192–1,587}$) was analyzed by SDS-PAGE and CBB staining.

(B) A schematic of the in vitro cohesin loading reaction.

(C) The gel image shows the recovered DNA from the cohesin-loading assay performed with the indicated concentrations of Mis4C$^{192–1,587}$ or Mis4/Ssl3. The graph shows the quantification of the results.

(D) Chromatin fractionation of budding yeast cells, synchronized in mitosis after depletion of endogenous Scc2. The levels of ectopic full-length or truncated Scc2 and of cohesin (Scc1) on chromatin were analyzed by western blotting. Tubulin and H3 served as loading controls for the whole-cell extract (WCE), supernatant (S), and chromatin pellet (P) fractions.

(E) DNA-binding activity of the constructs used for structural studies. Proteins at the indicated concentration were mixed with dsDNA and analyzed by gel electrophoresis.

mobility shift assay comparing the full-length Scc2-Scc4 complex, which has been shown to have a DNA-binding activity (Murayama and Uhlmann, 2014), with the Scc2N-Scc4 construct (Figure 3E). This shows that the Scc2N-Scc4 protein has no intrinsic affinity for DNA, suggesting chromatin interaction occurs via a protein receptor.

EM Analysis on the Scc2-Scc4 Complex

In order to study the overall structure of the Scc2-Scc4 complex and to gain insight into the loading mechanism of the cohesin ring, we performed negative-stain EM analysis on the 244-kDa Scc2-Scc4 complex. The complex was of a high degree of homogeneity judging from the quality of the micrographs and SDS-PAGE (Figure S1).

The 2D classes of Scc2-Scc4 reveal the tri-modular nature of the complex (Figures 4A and 4C). The complex is ~280 Å long (see below) with three distinct and sequential domains: (1) a globular head domain, (2) a central body consisting of two globular sub-structures, and (3) a hook-like tail domain. To assign the domains of the Scc2-Scc4 complex, a deletion study was performed using the 153-kDa Scc2C construct as a negative-stained EM sample. Scc2C, lacking the crystallized domain of Scc2N-Scc4, shows 2D class averages with striking details in the central body of the molecule and the hook-like domain while missing the large globular head domain that was seen in the full-length Scc2-Scc4 (Figures 4B and 4D). The large 100-Å globular head domain therefore corresponds to the crystallized Scc2N-Scc4 complex, which measures ~115 Å in length.

A distinct feature of the Scc2-Scc4 complex is that there is a high degree of flexibility between the three domains in relation to each other. The head domain, in particular can adopt a wide variety of angles with respect to the body of the complex (Figure 4E) suggesting that Scc2 forms an unstructured linker between the Scc4-binding domain and the central body. It is also apparent from the Scc2C class averages that the hook domain exhibits large conformational changes. This is a common feature among HEAT repeat proteins. For example, the protein phosphatase 2A A subunit changes from a twisted hook shape to a more closed horseshoe shape upon binding its C subunit (Cho and Xu, 2007). Based on the 2D class averages, the extended conformation of the hook can increase the length of the Scc2C domain from ~170 Å to ~280 Å. The switching between the extended and compact conformation of Scc2C may have important implications for the loading mechanism as discussed below.

DISCUSSION

Here, we provide atomic-resolution insights into the structure of the Scc2N-Scc4 cohesin loader complex. We have also uncovered the modular nature of the Scc2-Scc4 complex by EM analysis, which reveals a remarkable level of conformational flexibility. Previous studies have shown that the cohesin ring itself is highly flexible, with potential folding of the coiled coil at defined points (Huis in 't Veld et al., 2014). Analysis of the *S. pombe* cohesin loader, Mis4^{Scc2}-Ssl3^{Scc4} show that it is able to contact cohesin at several points around the circumference of the ring (Murayama and Uhlmann, 2014). The conformational flexibility of Scc2 implied by image analysis shows that the loader complex could potentially capture cohesin at multiple points around the ring and remain bound during the molecular gymnastics required to load the protein onto DNA. Given that the fully extended conformation of the loader is ~28 nm, whereas the cohesin ring is ~50 nm across, we suppose that cohesin is only productively bound by the loader when in a transiently "collapsed" configuration. Our in vitro cohesin-loading experiment reveal that the Scc2 N terminus and the Scc4 subunit are not required for catalyzing cohesin loading onto DNA. Instead, these domains are probably required for localizing the complex to its chromosomal receptor. The fact that several CdLS mutations map to the external surface of this domain, but likely do

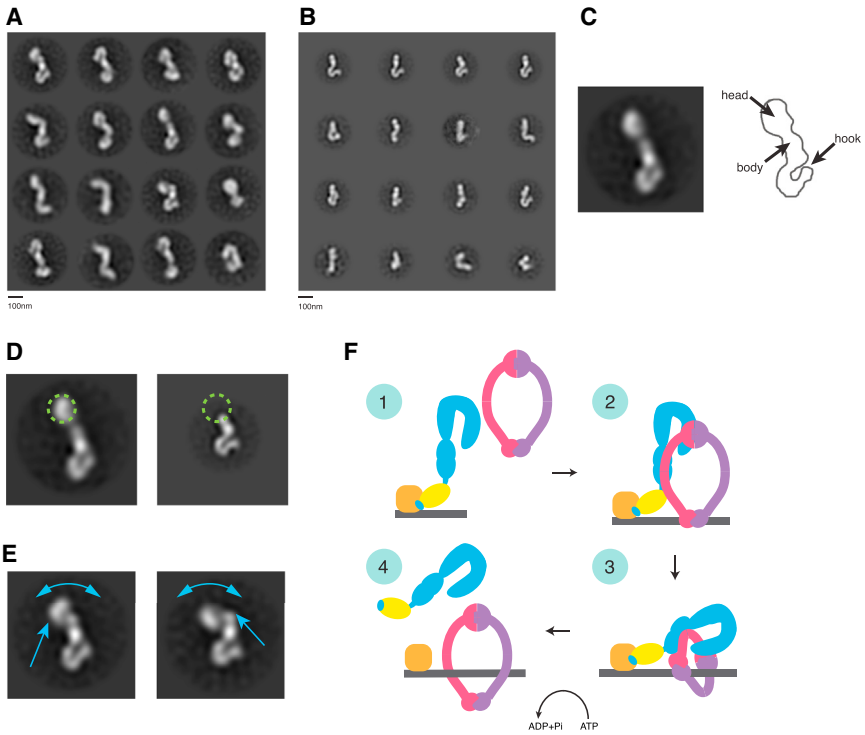

Figure 4. EM Studies on Scc2-Scc4

(A and B) Reference-free class averages of the full-length Scc2-Scc4 complex (A) and the Scc2 C-terminal domain (Scc2C) (B). Scale bar, 100 nm.

(C) The Scc2-Scc4 complex can be divided into a globular head domain, a central body, and a C-terminal hook domain.

(D) Class averages comparing the full-length Scc2-Scc4 and Scc2C unambiguously assign the globular head domain to be the crystallized Scc2N-Scc4 complex.

(E) A large degree of flexibility can be observed along the Scc2-Scc4 molecule, with both the head and the hook domains being flexible in relation to the central body. The head domain can rotate through almost 180° with respect to the body around a hinge region (blue arrow). See also Figure S2.

(F) Schematics of a speculative Scc2-Scc4-mediated cohesin loading mechanism. The mechanism is described in the Discussion. The Scc2-Scc4 complex is depicted in blue and yellow, cohesin in purple and red, and the chromatin receptor in brown.

not affect complex formation per se, lends support to this argument. However, our results show that Scc4 is required for efficient chromatin targeting in vivo.

If Scc4 represents a targeting subunit to localize the loader to chromosomes, then what is its target? Previous studies with the fission yeast Mis4^{Scc2}-Ssl3^{Scc4} proteins have attributed a DNA-binding activity to Mis4, but not Ssl3 (Murayama and Uhlmann, 2014), which is recapitulated with our constructs. Examination of the Scc4 crystal structure provides few clues, but the presence of an extremely highly conserved external grooved ridge is indicative of a protein-protein interface. In *Xenopus*, localization of Scc2 to pre-replication complexes has been proposed to occur via an interaction with the Cdc7-Drf1 (DDK) kinase (Takahashi et al., 2008), while in yeast, the Ctf19/COMA complex has been shown to be required for enrichment of Scc2-Scc4 in the pericentromere (Fernius et al., 2013), also possibly via DDK (Natsume et al., 2013). However, despite extensive efforts, we were unable to detect a direct interaction with yeast Cdc7-Dbf4, Ctf19/COMA, or the Chl4-Iml1 complex using recombinant proteins in pull-down assays (data not shown). These results may reflect limitations of our experimental approach or species-specific differences or suggest the requirement of additional factors to explain the in vivo results.

Together with previously identified Scc2-Scc4 interaction sites on cohesin subunits (Murayama and Uhlmann, 2014), we can hypothesize a cohesin loading mechanism which requires a large conformation change in the cohesin ring that is mediated by the Scc2-Scc4 complex (Figure 4F). First, Scc2-Scc4 localizes onto chromosome by recognizing various chromatin-localized receptors via either Scc2 N terminus, Scc4, or both subunits. The transition of the compact to extended conformation of the Scc2 C terminus allows the Scc2-Scc4 complex to capture the cohesin ring spanning both the hinge and head region. Subsequently, the Scc2-Scc4-cohesin supercomplex transiently adopts a compact conformation, which brings the head domain into close proximity with the hinge domain, possibly driven by ATP binding to the Smc nucleotide-binding domains (NBDs) affecting coiled-coil geometry. Similar nucleotide-induced conformational transitions have been postulated to occur in related ABC ATPases such as the Rad50 protein (Lammens et al., 2011; Williams et al., 2011). This conformational change may trigger the opening of the cohesin ring to allow DNA access. Upon ATP hydrolysis by the NBDs, the Scc2-Scc4 complex can be released from cohesin, which in turns closes and entraps the DNA. The freed Scc2-Scc4 can catalyze more loading of cohesin onto chromosome.

We also note that the extreme flexibility of the head domain provides an explanation for the proteolytic susceptibility of the Scc2 N terminus previously reported (Woodman et al., 2014) as well as our own limited proteolysis results. Interestingly, we identified several potential Cdk sites [S/T]PX[K/R] around the area susceptible to proteolysis (Figure S2). Since it has been shown that phosphorylation at Cdk sites contributes to structural stability in the retinoblastoma protein (Burke et al., 2012) and in Cdh1 inhibitor Acm1 (He et al., 2013), it remains a possibility that cell-cycle-dependent phosphorylation events affect the flexibility of the Scc2-Scc4 complex and modulate its activity.

Although this article was in revision, the crystal structure of the *S. cerevisiae* Scc4-Scc2N complex was described (Hinshaw et al., 2015). The overall folds of the two structures are comparable, with a small difference in the interactions between the end of the N-terminal helix of Scc4 with Scc2. Given that these regions are well defined in electron density maps, these probably reflect species-specific adaptations.

EXPERIMENTAL PROCEDURES

Cloning and Protein Purification

Ashbya gossypii SCC2 and SCC4 were amplified by PCR from genomic DNA (LGC Standards) and cloned into a modified version of the MultiBac vector pFBDM (Fitzgerald et al., 2006; Zhang et al., 2013). A double Strep-tag II (ds) and TEV protease cleavage site were introduced into the N terminus of Scc2. The resultant protein expression cassettes were recombined in DH10MultiBac cells to create a bacmid. The ds–Scc2-Scc4 complex was expressed using the baculovirus and insect cell (High 5 cells) systems and purified by a combination of Strep-Tactin (QIAGEN), anion exchange chromatography Resource Q, and Superdex 200 size-exclusion chromatography (GE Healthcare). Proteolytic products of both proteins were observed in the purified samples and subsequently identified by mass spectrometry. The shorted products were re-cloned and purified using protocols identical to those used for the full-length proteins.

Crystallization

Crystals were grown by sitting-drop vapor diffusion. Protein at 5 mg/ml was mixed with crystallization solution, 100 mM sodium cacodylate (pH 6.5), 200 mM calcium acetate, 13% polyethylene glycol 6000, and 20% glycerol at 20°C. Crystals grew to full size after 1 week and were flash-cooled in liquid nitrogen.

Structure Solution

The structure of the Scc4-Scc2 complex was solved by multiple-wavelength anomalous dispersion using a selenomethionine-substituted protein. Native data were collected on beamline IO4-1 at the Diamond Light Source and a three-wavelength selenomethionine dataset on beamline BM30A at the ESRF. The structure was solved using the AutoSHARP package (Bricogne et al., 2003), and an initial model was traced using Buccaneer (Cowtan, 2006). Iterative rounds of rebuilding and refinement were carried out using Coot (Emsley and Cowtan, 2004) and phenix.refine (Adams et al., 2010). Final refinement was carried out against a native dataset at 2.6 Å. Full data collection and refinement statistics are given in Table S1.

EM

Samples of the intact Scc2-Scc4 complex and Scc2C were applied to glow-discharged carbon-coated Quantifoil 2/2 grids at ~10 ng/μl and stained with 2% uranyl formate. Grids were visualized on a Tecnai G2 electron microscope operating at 120 kV. Images were recorded on a Gatan Orius SC1000 camera at 26,000× magnification giving a final sampling of 2.63 Å/pixel (full-length complex) or a Gatan Ultrascan 2K at 30,000×, 3.45 Å/pixel (Scc2C).

Image Processing

Particles were manually picked for each dataset using the EMAN2 package (Tang et al., 2007). 2,936 particles of the full-length complex and 5,191 of the Scc2 C-terminal comprised each set. Reference-free class averages were calculated with Relion (Scheres, 2012).

In Vitro Cohesin Loading Assay

The fission yeast Scc2C$^{192–1,587}$ (Mis4C^{V}) and cohesin complex/Psc3 were purified and assayed using previously described protocols (Murayama and Uhlmann, 2014). The indicated concentration of Mis4/Ssl3 or Mis4C$^{192–1,587}$ was mixed with 150 nM cohesin, 100 nM Psc3, and 3.3 nM relaxed circular DNA (pBluescript KSII (+)) in the reaction buffer on ice. The reaction was initiated by addition of 0.5 mM ATP and incubated at 32°C for 1 hr. The DNA-cohesin complex was retrieved by immunoprecipitation, and the bound DNA was analyzed by agarose gel electrophoresis.

In Vivo Chromatin-Binding Assay

Budding yeast cells were grown in synthetic medium (YNB) lacking methionine to maintain endogenous Scc2 expression that was placed under control of the *MET3* promoter. α-Factor was added to arrest cells in G1, and after 1.5 hr, the culture was transferred to YPD medium to repress Scc2 expression and 88 μg/ml indoleacetic acid (IAA) was added to initiate Scc2 degradation. After a further 2 hr, cells were released from the G1 block into YPD medium containing IAA and 5 μg/ml nocodazole. 2 hr after release, when the cultures were uniformly arrested in mitosis, cell extracts were prepared and separated into soluble and chromatin-bound fractions. These were analyzed by SDS-PAGE and western blotting. Cell-cycle synchrony was confirmed by FACS analysis of DNA content (not shown). Strains are listed in Table S2.

DNA-Binding Assay

Full-length Scc2-Scc4 or Scc2N-Scc4 was incubated with 150 fmol 700 bp mixed-sequence DNA. Samples were electrophoresed on a 0.8% agarose gel and DNA visualized by subsequent ethidium bromide staining.

ACCESSION NUMBERS

Structure factors and coordinates for Scc4-Scc2N have been deposited in the Protein Data Bank under accession code PDB: 5C6G.

SUPPLEMENTAL INFORMATION

Supplemental Information includes seven figures and two tables and can be found with this article online at 10.1016/j.celrep.2015.06.071.

AUTHOR CONTRIBUTIONS

W.C.H.C. and M.R.S. conceived the study, determined the crystal structure of Scc2N-Scc4, and co-wrote the manuscript. Y.M. performed the in vitro cohesin-loading assay. S.M. carried out the in vivo experiments. W.C.H.C., A.C., and M.R.S. performed the EM analysis. All authors contributed to experimental design and provided editorial input for the manuscript.

ACKNOWLEDGMENTS

We thank A. Purkiss for providing assistance in crystal data collection, R. Carzaniga and the LRI EM Unit for assistance with microscopy, and D. Frith (LRI Protein Analysis Unit) for performing mass spectrometry fingerprint experiments. This work was supported by the Francis Crick Institute, which receives its core funding from Cancer Research UK, the UK Medical Research Council, and the Wellcome Trust.

Received: May 26, 2015
Revised: June 22, 2015
Accepted: June 26, 2015
Published: July 23, 2015

REFERENCES

Adams, P.D., Afonine, P.V., Bunkóczi, G., Chen, V.B., Davis, I.W., Echols, N., Headd, J.J., Hung, L.-W., Kapral, G.J., Grosse-Kunstleve, R.W., et al. (2010). PHENIX: a comprehensive Python-based system for macromolecular structure solution. Acta Crystallogr. D Biol. Crystallogr. *66*, 213–221.

Bernard, P., Drogat, J., Maure, J.F., Dheur, S., Vaur, S., Genier, S., and Javerzat, J.P. (2006). A screen for cohesion mutants uncovers Ssl3, the fission yeast counterpart of the cohesin loading factor Scc4. Curr. Biol. *16*, 875–881.

Bricogne, G., Vonrhein, C., Flensburg, C., Schiltz, M., and Paciorek, W. (2003). Generation, representation and flow of phase information in structure determination: recent developments in and around SHARP 2.0. Acta Crystallogr. D Biol. Crystallogr. *59*, 2023–2030.

Burke, J.R., Hura, G.L., and Rubin, S.M. (2012). Structures of inactive retinoblastoma protein reveal multiple mechanisms for cell cycle control. Genes Dev. *26*, 1156–1166.

Cho, U.S., and Xu, W. (2007). Crystal structure of a protein phosphatase 2A heterotrimeric holoenzyme. Nature *445*, 53–57.

Ciosk, R., Shirayama, M., Shevchenko, A., Tanaka, T., Toth, A., Shevchenko, A., and Nasmyth, K. (2000). Cohesin's binding to chromosomes depends on a separate complex consisting of Scc2 and Scc4 proteins. Mol. Cell *5*, 243–254.

Cowtan, K. (2006). The Buccaneer software for automated model building. 1. Tracing protein chains. Acta Crystallogr. D Biol. Crystallogr. *62*, 1002–1011.

Dorsett, D. (2011). Cohesin: genomic insights into controlling gene transcription and development. Curr. Opin. Genet. Dev. *21*, 199–206.

Emsley, P., and Cowtan, K. (2004). Coot: model-building tools for molecular graphics. Acta Crystallogr. D Biol. Crystallogr. *60*, 2126–2132.

Fernius, J., Nerusheva, O.O., Galander, S., Alves, Fde.L., Rappsilber, J., and Marston, A.L. (2013). Cohesin-dependent association of scc2/4 with the centromere initiates pericentromeric cohesion establishment. Curr. Biol. *23*, 599–606.

Fitzgerald, D.J., Berger, P., Schaffitzel, C., Yamada, K., Richmond, T.J., and Berger, I. (2006). Protein complex expression by using multigene baculoviral vectors. Nat. Methods *3*, 1021–1032.

Gillespie, P.J., and Hirano, T. (2004). Scc2 couples replication licensing to sister chromatid cohesion in Xenopus egg extracts. Curr. Biol. *14*, 1598–1603.

Haering, C.H., Farcas, A.M., Arumugam, P., Metson, J., and Nasmyth, K. (2008). The cohesin ring concatenates sister DNA molecules. Nature *454*, 297–301.

He, J., Chao, W.C.H., Zhang, Z., Yang, J., Cronin, N., and Barford, D. (2013). Insights into degron recognition by APC/C coactivators from the structure of an Acm1-Cdh1 complex. Mol. Cell *50*, 649–660.

Hinshaw, S.M., Makrantoni, V., Kerr, A., Marston, A.L., and Harrison, S.C. (2015). Structural evidence for Scc4-dependent localization of cohesin loading. eLife *4*, 4.

Huis in 't Veld, P.J., Herzog, F., Ladurner, R., Davidson, I.F., Piric, S., Kreidl, E., Bhaskara, V., Aebersold, R., and Peters, J.M. (2014). Characterization of a DNA exit gate in the human cohesin ring. Science *346*, 968–972.

Kagey, M.H., Newman, J.J., Bilodeau, S., Zhan, Y., Orlando, D.A., van Berkum, N.L., Ebmeier, C.C., Goossens, J., Rahl, P.B., Levine, S.S., et al. (2010). Mediator and cohesin connect gene expression and chromatin architecture. Nature *467*, 430–435.

Krantz, I.D., McCallum, J., DeScipio, C., Kaur, M., Gillis, L.A., Yaeger, D., Jukofsky, L., Wasserman, N., Bottani, A., Morris, C.A., et al. (2004). Cornelia de Lange syndrome is caused by mutations in NIPBL, the human homolog of Drosophila melanogaster Nipped-B. Nat. Genet. *36*, 631–635.

Kuzniacka, A., Wierzba, J., Ratajska, M., Lipska, B.S., Koczkowska, M., Malinowska, M., and Limon, J. (2013). Spectrum of NIPBL gene mutations in Polish patients with Cornelia de Lange syndrome. J. Appl. Genet. *54*, 27–33.

Lammens, K., Bemeleit, D.J., Möckel, C., Clausing, E., Schele, A., Hartung, S., Schiller, C.B., Lucas, M., Angermüller, C., Söding, J., et al. (2011). The Mre11:Rad50 structure shows an ATP-dependent molecular clamp in DNA double-strand break repair. Cell *145*, 54–66.

Lengronne, A., Katou, Y., Mori, S., Yokobayashi, S., Kelly, G.P., Itoh, T., Watanabe, Y., Shirahige, K., and Uhlmann, F. (2004). Cohesin relocation from sites of chromosomal loading to places of convergent transcription. Nature *430*, 573–578.

Lightfoot, J., Testori, S., Barroso, C., and Martinez-Perez, E. (2011). Loading of meiotic cohesin by SCC-2 is required for early processing of DSBs and for the DNA damage checkpoint. Curr. Biol. *21*, 1421–1430.

Lopez-Serra, L., Kelly, G., Patel, H., Stewart, A., and Uhlmann, F. (2014). The Scc2-Scc4 complex acts in sister chromatid cohesion and transcriptional regulation by maintaining nucleosome-free regions. Nat. Genet. *46*, 1147–1151.

Murayama, Y., and Uhlmann, F. (2014). Biochemical reconstitution of topological DNA binding by the cohesin ring. Nature *505*, 367–371.

Muto, A., Ikeda, S., Lopez-Burks, M.E., Kikuchi, Y., Calof, A.L., Lander, A.D., and Schilling, T.F. (2014). Nipbl and mediator cooperatively regulate gene expression to control limb development. PLoS Genet. *10*, e1004671.

Natsume, T., Müller, C.A., Katou, Y., Retkute, R., Gierliński, M., Araki, H., Blow, J.J., Shirahige, K., Nieduszynski, C.A., and Tanaka, T.U. (2013). Kinetochores coordinate pericentromeric cohesion and early DNA replication by Cdc7-Dbf4 kinase recruitment. Mol. Cell *50*, 661–674.

Neuwald, A.F., and Hirano, T. (2000). HEAT repeats associated with condensins, cohesins, and other complexes involved in chromosome-related functions. Genome Res. *10*, 1445–1452.

Nishimura, K., Fukagawa, T., Takisawa, H., Kakimoto, T., and Kanemaki, M. (2009). An auxin-based degron system for the rapid depletion of proteins in nonplant cells. Nat. Methods *6*, 917–922.

Scheres, S.H.W. (2012). RELION: implementation of a Bayesian approach to cryo-EM structure determination. J. Struct. Biol. *180*, 519–530.

Seitan, V.C., Banks, P., Laval, S., Majid, N.A., Dorsett, D., Rana, A., Smith, J., Bateman, A., Krpic, S., Hostert, A., et al. (2006). Metazoan Scc4 homologs link sister chromatid cohesion to cell and axon migration guidance. PLoS Biol. *4*, e242.

Takahashi, T.S., Basu, A., Bermudez, V., Hurwitz, J., and Walter, J.C. (2008). Cdc7-Drf1 kinase links chromosome cohesion to the initiation of DNA replication in Xenopus egg extracts. Genes Dev. *22*, 1894–1905.

Tang, G., Peng, L., Baldwin, P.R., Mann, D.S., Jiang, W., Rees, I., and Ludtke, S.J. (2007). EMAN2: an extensible image processing suite for electron microscopy. J. Struct. Biol. *157*, 38–46.

Tonkin, E.T., Wang, T.J., Lisgo, S., Bamshad, M.J., and Strachan, T. (2004). NIPBL, encoding a homolog of fungal Scc2-type sister chromatid cohesion proteins and fly Nipped-B, is mutated in Cornelia de Lange syndrome. Nat. Genet. *36*, 636–641.

Watrin, E., Schleiffer, A., Tanaka, K., Eisenhaber, F., Nasmyth, K., and Peters, J.M. (2006). Human Scc4 is required for cohesin binding to chromatin, sister-chromatid cohesion, and mitotic progression. Curr. Biol. *16*, 863–874.

Williams, G.J., Williams, R.S., Williams, J.S., Moncalian, G., Arvai, A.S., Limbo, O., Guenther, G., SilDas, S., Hammel, M., Russell, P., and Tainer, J.A. (2011). ABC ATPase signature helices in Rad50 link nucleotide state to Mre11 interface for DNA repair. Nat. Struct. Mol. Biol. *18*, 423–431.

Woodman, J., Fara, T., Dzieciatkowska, M., Trejo, M., Luong, N., Hansen, K.C., and Megee, P.C. (2014). Cell cycle-specific cleavage of Scc2 regulates its cohesin deposition activity. Proc. Natl. Acad. Sci. USA *111*, 7060–7065.

Zhang, Z., Yang, J., Kong, E.H., Chao, W.C., Morris, E.P., da Fonseca, P.C., and Barford, D. (2013). Recombinant expression, reconstitution and structure of human anaphase-promoting complex (APC/C). Biochem. J. *449*, 365–371.